A novel robust disturbance rejection anti-windup framework

Guang Li *, Guido Herrmann†, David P. Stoten†, Jiaying Tu †
and Matthew C. Turner ‡

November 25, 2010

Abstract

In this paper, we propose a novel anti-windup (AW) framework for coping with input saturation in the disturbance rejection problem of stable plant systems. This framework is based on the one developed by Weston and Postlethwaite (W&P) [26]. The new AW-design improves the disturbance rejection performance over the design framework usually suggested for the coprime-factorization based W&P-approach. Performance improvement is achieved by explicitly incorporating a transfer function, which represents the effect of the disturbance on the nonlinear loop, into the AW compensator synthesis. An extra degree of freedom is exploited for the coprime factorization, resulting in an implicitly computed multivariable algebraic loop for the AW-implementation. Suggestions are made to overcome the algebraic loop problem via explicit computation. Furthermore, paralleling the results of former

*G. Li is with the School of Engineering, Mathematics and Computing, The University of Exeter, g.li@ex.ac.uk. This work was completed when G. Li was with the Advanced Control and Test Laboratory (ACTLab), Department of Mechanical Engineering, University of Bristol.

†G. Herrmann, D. P. Stoten and J. Tu are with the ACTLab, Department of Mechanical Engineering, University of Bristol, Queens Building, University Walk, Bristol, BS8 1TR, UK. {g.herrmann, d.p.stoten, jiaying.tu}@bristol.ac.uk

‡M. C. Turner is with the Control and Instrumentation Research Group, Department of Engineering, University of Leicester, University Road, Leicester, LE1 7RH, UK, mct6@le.ac.uk

work [23], the additive plant uncertainty is incorporated into the AW compensator synthesis, by using a novel augmentation for the disturbance rejection problem. In this new framework, it is shown that the internal model control (IMC) scheme is optimally robust, as was the case in [23, 29].

The new AW approach is applied to the control of dynamically substructured systems (DSS) subject to external excitation signals and actuator limits. The benefit of this approach is demonstrated in the simulations for a small-scale building mass damper DSS and a quasi-motorcycle DSS.

1 Introduction

To improve the stability and performance of control systems subject to control input saturation, anti-windup (AW) control has been extensively studied, see, e.g., [1–3, 11, 12, 22, 23, 26, 28]. The main feature of this strategy is that a two-step design procedure is involved in the controller synthesis: a nominal (linear) controller is initially designed whilst ignoring the input saturation; then, a linear compensator is synthesized to cope with the windup problem. Among the existing AW approaches, the linear conditioning scheme proposed by Weston and Postlethwaite (W&P) [26] is comparatively easy to implement. Its design objective is to recover the system's linear behaviour quickly, when input saturation occurs. Successful applications of the W&P scheme to aerospace, hard-disk drive and wireless network problems have been reported (see, e.g., [5, 6, 25]).

Current studies of the W&P scheme mainly focus on stability and the recovery of linear control performance for tracking problems. However, disturbances are always present and can deteriorate performance significantly. Hence, although it is not necessary to consider the disturbances when studying the system stability alone, the system performance in the presence of disturbances is nontrivial and has received scant attention in the W&P literature.

This paper aims to develop an AW framework for the disturbance rejection problem based on the W&P scheme. Performance is improved by explicitly incorporating a transfer function, representing the effect of the disturbance on the nonlinear loop, into the AW synthesis. The incorporation of this transfer function requires an extra matrix variable

when using the Projection Lemma to synthesize the AW compensator. Unfortunately, this variable introduces an algebraic loop into the framework and we propose a generic method that resolves this algebraic loop, which has its potential applications in a range of situations. Furthermore, additive uncertainty in the plant is also incorporated into the synthesis, which enables a tradeoff between AW performance and robustness. This provides an alternative to the result in [23].

In addition, we focus on an application of the new AW-design in a field of current worldwide interest, i.e. the problem of dynamically substructured systems (DSS), for real-time experimental dynamics tests (see, e.g., [15, 18] and the references therein). The DSS approach allows for critical engineering components, called physical substructures, to be tested at full size, while the remaining parts of the system, called numerical substructures, are run in real-time simultaneously. This approach can overcome drawbacks involved with purely numerical or purely physical testing. On the one hand, some physical components may contain significant uncertainties and nonlinearities, so that replacing them by an estimated numerical model may greatly influence the testing results. In particular, it is possible to test safety-critical physical components; for example, a numerical aerodynamic model can be used to add a vertical force and pitch moment to the body of physical racing car in a track simulation test rig, so that the aerodynamics of the racing car can be investigated [16]. On the other hand, using some physical components in a testing procedure may be either unnecessary or unrealistic (e.g., the inclusion of a full-size dam or bridge within a laboratory environment). See [18, 27] for a detailed discussion on the advantages of using DSS. The control objective in DSS is to synchronize the interaction signals at the interface between the numerical and physical substructures, subject to the testing (excitation) signal. Since the testing signal for the DSS in the controller design can be assumed to be a measured disturbance, DSS control is essentially a regulation problem with measured disturbance attenuation. Normally, DSS are designed so that actuator limits are not an issue. However, actuator saturation can occur in some DSS implementations, in which case synchronization would be lost and the test be invalidated. Therefore, the study of AW-design is important for DSS in such circumstances. We use two DSS simulation examples to show the advantage of the new AW approach developed

in this paper.

The structure of this paper is as follows. Notation is summarized in section 2. Then, the generic framework for the disturbance rejection AW-compensator design is proposed in section 3: the nominal case is considered in subsection 3.1; in subsection 3.2, this approach is further extended to the design of the robust AW-compensator for the disturbance rejection problem, by incorporating additive uncertainty. The algebraic loop problem associated with this approach is resolved in section 4. Section 5 presents two comparative AW approaches, for completeness. In section 6, the AW approach, together with the comparator methods, are applied to two DSS systems in numerical simulations. Finally, section 7 concludes the paper.

2 Notation

Let $\mathcal{T}$ denote an operator or mapping. Then $\|\mathcal{T}\|_\infty$ denotes the $\mathcal{H}_\infty$ norm of a linear operator $\mathcal{T}$ and the induced $\mathcal{L}_2$ norm of a nonlinear operator $\mathcal{T}$ is defined as

$$\|\mathcal{T}\|_{i,2} := \sup_{\|x\|_2 \neq 0} \frac{\|\mathcal{T}x\|_2}{\|x\|_2} \tag{1}$$

where $\|x\|_2 := \sqrt{\int_0^\infty \|x\|^2 dt}$ is the $\mathcal{L}_2$ norm with $\|x\| := \sqrt{\sum_{i=1}^n |x_i|^2}$ as the Euclidean norm.

A n by n matrix D is diagonal if its entries $d_{ij} = 0$ for $j \neq i$. We denote a diagonal matrix as $D = \text{diag}(d_{11}, \ldots, d_{nn})$ or $D = \text{diag}(d)$, where d is the vector of diagonal entries of D.

The single-variable signum function is defined as

$$\text{sign}(u_i) = \begin{cases} 1 & \text{for } u_i > 0 \\ 0 & \text{for } u_i = 0 \\ -1 & \text{for } u_i < 0 \end{cases}.$$

and the multi-variable signum function for a vector u is:

$$\text{Sign}(u) = \text{diag}\left(\text{sign}(u_1), \text{sign}(u_2), \cdots, \text{sign}(u_m)\right)$$

The multi-variable saturation function is defined as

$$\text{Sat}(u) := [\text{sat}_1(u_1), \ldots, \text{sat}_m(u_m)]^T \tag{2}$$

where $\text{sat}_i(u_i) := \text{sign}(u_i) \times \min\{|u_i|, \bar{u}_i\}$ and $\bar{u}_i > 0$ is the i'th saturation limit. The following identity holds

$$\text{Dz}(u) = u - \text{Sat}(u) \tag{3}$$

where $\text{Dz}(u)$ is the deadzone function. The deadzone operator

$$\text{Dz}(u) = [\text{dz}_1(u_1), \text{dz}_2(u_2), \cdots, \text{dz}_m(u_m)]^T$$

where $\text{dz}_i(u_i) = \text{sign}(u_i)\max(|u_i| - \bar{u}_i, 0)$ can be subject to differing limit values $\bar{u} = [\bar{u}_1, \bar{u}_2, \cdots, \bar{u}_m]^T$.

A decentralized nonlinear element $\mathcal{N}(\cdot) = \text{diag}(n_1(\cdot), \ldots, n_m(\cdot))$ is said to belong to the Sector$[0, I]$ if all $n_i(\cdot)$ belong to the Sector$[0, 1]$, that is:

$$0 \leq u_i n_i(u_i) \leq u_i^2, \ u_i \in \mathbb{R}. \tag{4}$$

Hence, this implies for any $n_i(\cdot)$

$$n_i^2(u_i) \leq u_i n_i(u_i) \leq u_i^2. \tag{5}$$

Note that both the saturation and deadzone operators belong to Sector$[0, I]$. For a decentralised Sector$[0, I]$ nonlinearity, it follows that there exists a diagonal matrix W such that

$$\mathcal{N}(u)'W(u - \mathcal{N}(u)) \geq 0, \ u \in \mathbb{R}^m \tag{6}$$

Let a matrix $E \in \mathbb{R}^{n\times n}$, and denote its entries as e_{ij}. Then the matrix E is said to be strictly diagonally dominant (see page 349 in [8]) if

$$|e_{ii}| > \sum_{j\neq i} |e_{ij}| \quad \text{for all } i = 1, \ldots, n$$

3 A generic framework for the disturbance rejection anti-windup compensator

The AW scheme we employ is inspired by the framework proposed by [23, 26], as shown in Fig. 1. The transfer functions for the plant and controller are

$$\mathcal{P}(s) = \begin{bmatrix} \mathcal{P}_w(s) & \mathcal{P}_u(s) \end{bmatrix} \qquad \mathcal{K}(s) = \begin{bmatrix} \mathcal{K}_w(s) & \mathcal{K}_y(s) \end{bmatrix} \tag{7}$$

where all the uncertainties from u_{lin} to y_{lin} are assumed to be lumped into an additive uncertainty, represented by a stable transfer function $\Delta(s)$.

The results in this section are based on the two assumptions of which the first one concerns the open loop plant:

Assumption 1 *$\mathcal{P}_u$ (and P_w) is asymptotically stable.*

If the right coprime factorization of $\mathcal{P}_u(s)$ is $\mathcal{P}_u(s) = (N(s)E)(M(s)E)^{-1}$, so that

$$\begin{bmatrix} M(s)E - I \\ N(s)E \end{bmatrix} \sim \left[\begin{array}{c|c} A_p + B_pF & B_pE \\ \hline F & E - I \\ C_p + D_pF & D_pE \end{array}\right] \tag{8}$$

then the system conditioning in Fig. 1 is achieved by tuning F and E. Via block diagram manipulation, Fig. 1 can be equivalently represented by Fig. 2, which allows us to study system stability and performance in an easier way. In [26], the concept of minimizing the $\mathcal{L}_2$ gain from u_{lin} to y_d for AW-compensator design is proposed, and in [23] this concept is further extended by incorporating an additive uncertainty of the plant into the AW-compensator synthesis through minimizing an extra term from u_{lin} to z_Δ.

In this paper, we aim to reduce the influence of the external disturbance signal $\tilde{d}$. Hence the control objective is modified by minimizing the $\mathcal{L}_2$ gain from the external signal $\tilde{d}$ to y_d directly. To do this, an extra transfer function $\mathcal{P}_d$ from $\tilde{d}$ to u_{lin} is included, so that Fig. 2 can be simplified to Fig. 3 for the AW-compensator design. In Fig. 3, the states of $\mathcal{P}_d$ and $\mathcal{P}_u$ are $x_d \in \mathbb{R}^{n_d}$ and $x_p \in \mathbb{R}^{n_p}$; the dimensions of the signals and matrices are $u_{\text{lin}}, u_d, \tilde{u} \in \mathbb{R}^{n_u}$, $y_d \in \mathbb{R}^{n_y}$, $E \in \mathbb{R}^{n_u \times n_u}$ and $F \in \mathbb{R}^{n_u \times n_p}$.

The transfer function from $\tilde{d} = d$ to u_{lin} in Fig. 2 is derived as $\mathcal{P}_d(s) = (I - \mathcal{K}_y\mathcal{P}_u)^{-1}(\mathcal{K}_w + \mathcal{K}_y\mathcal{P}_w) \sim (A_d, B_d, C_d, D_d)$. This implies another assumption, the nominal closed loop:

Assumption 2 *$\mathcal{P}_d$ is well-posed and asymptotically stable.*

Assumptions 1 and 2 are sufficient and standard assumptions made in constrained control to achieve global stability [22, 23].

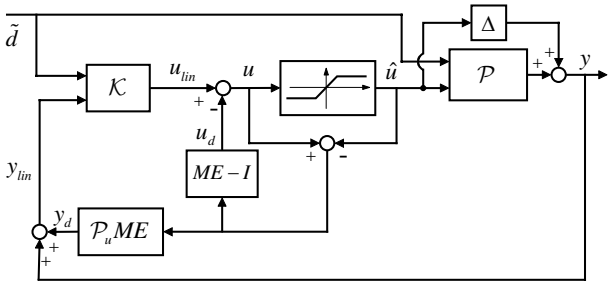

Figure 1: Anti-windup scheme

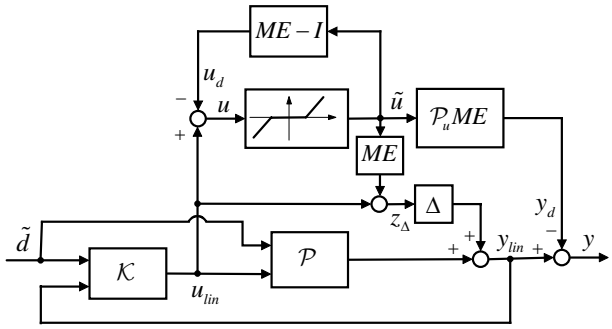

Figure 2: Equivalent representation of Fig. 1

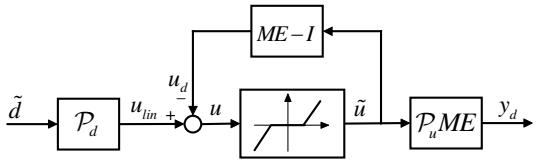

Figure 3: Anti-windup framework for disturbance rejection

3.1 Design of AW-compensators for disturbance rejection (DAW)

We first consider the nominal case, where the additive uncertainty is not present and the disturbance signal $\tilde{d} = d$. Given the AW framework as shown in Fig. 3, we have the following theorem for AW compensator synthesis:

Theorem 1 *The $\mathcal{L}_2$ gain from d to y_d is less than γ_d if there exists a symmetric positive definite matrix*

$$P := \begin{bmatrix} P_{11} & P_{12} \\ P_{12}^T & P_{22} \end{bmatrix} \in \mathbb{R}^{n_p+n_d} \tag{9}$$

such that the following two linear matrix inequalities (LMIs) are satisfied

$$\begin{bmatrix} PA_o + A_o^T P + PW_A + W_A^T P & W_C + PW_B \\ W_C^T + W_B^T P & W_D \end{bmatrix} < 0 \tag{10}$$

with

$$A_o = \begin{bmatrix} A_p & 0 \\ 0 & A_d \end{bmatrix} \tag{11}$$

$$W_A = \begin{bmatrix} 0_{n_p} & B_p C_d \\ 0_{n_d \times n_p} & 0_{n_d} \end{bmatrix} \qquad W_B = \begin{bmatrix} B_p D_d & 0_{n_p \times n_y} \\ B_d & 0_{n_d \times n_y} \end{bmatrix}$$

$$W_C = \begin{bmatrix} 0_{n_p \times n_w} & C_p^T \\ 0_{n_d \times n_w} & C_d^T D_p^T \end{bmatrix} \qquad W_D = \begin{bmatrix} -\gamma_d I_{n_w} & D_d^T D_p^T \\ D_p D_d & -\gamma_d I_{n_y} \end{bmatrix}$$

and

$$\begin{bmatrix} A_d^T P_{22} + P_{22} A_d & P_{22} B_d \\ B_d^T P_{22} & -\gamma_d I_{n_w} \end{bmatrix} < 0 \tag{12}$$

with $\gamma_d > 0$.

Proof The proof can be developed using the Projection Lemma, by following similar approaches to those given in, e.g. [3, 7]. See the Appendix for details. □

Remark 1 It has been shown that the framework of W&P falls into the more generic one of Grimm *et al.* [3], but the W&P framework is much less complicated to implement [7]. Theorem 1 in this paper, as an extension of the W&P framework, can also be subsumed into the framework of Grimm *et al.* [3]; the emphasis here is the parameterization of

the AW compensator via a coprime factorization approach, which is simpler and more tractable than [3].

Remark 2 It is possible to further reduce the stability conservatism by using other conditions on the saturation/deadzone, e.g. [9, 13], although the design complexity might be increased.

Remark 3 We summarize the AW compensator synthesis procedure as follows:

1) Given the matrix variable $P = P^T > 0$, solve $\gamma_d^* := \min \gamma_d > 0$ subject to LMIs (10) and (12) to yield P^* and γ_d^*.

2) Substituting P^* and γ_d^* with some chosen diagonal positive definite W, solve the LMI:

$$\Psi + H^T \Lambda G + G^T \Lambda^T H < 0 \tag{13}$$

for Λ, with $\Lambda := \begin{bmatrix} F & E \end{bmatrix}$ and

$$\Psi = \begin{bmatrix} A_o^T P + P A_o & P B_o + C_{do}^T \tilde{W} & C_{po}^T \\ B_o^T P + \tilde{W} C_{do} & \tilde{W} D_{do} + D_{do}^T \tilde{W} - \gamma_d \tilde{I}_{n_w} & 0 \\ C_{po} & 0 & -\gamma_d I_{n_y} \end{bmatrix} \tag{14}$$

$$H = \left[\begin{array}{cc|cc|c} B_p^T & 0_{n_u \times n_d} & -I_{n_u} & 0_{n_u \times n_w} & D_p^T \end{array}\right] \mathrm{diag}(P, \tilde{W}, I) \tag{15}$$

$$G = \left[\begin{array}{cc|cc|c} I_{n_p} & 0_{n_p \times n_d} & 0_{n_p \times n_u} & 0_{n_p \times n_w} & 0_{n_p \times n_y} \\ 0_{n_u \times n_p} & 0_{n_u \times n_d} & I_{n_u} & 0_{n_u \times n_w} & 0_{n_u \times n_y} \end{array}\right] \tag{16}$$

$$\tilde{W} = \begin{bmatrix} W & 0 \\ 0 & I_{n_w} \end{bmatrix} \tag{17}$$

Remark 4 From the above AW compensator synthesis procedure, it can be seen that the poles of the AW compensator, i.e. the eigenvalues of $A_p + B_p F$, are mainly determined by the dynamics of $\mathcal{P}_d$ and $\mathcal{P}_u$. In section 3.2, an extra mapping representing robustness is involved in the $\mathcal{L}_2$ gain minimization, so that the poles can be placed more flexibly and a tradeoff between robustness and performance can be achieved.

Note that in Theorem 1, the Lyapunov function candidate with the form of $V(x_p, x_d) = [x_p^T, x_d^T]P[x_p^T, x_d^T]^T$ is used. If we simplify this Lyapunov function candidate to

$$V = x_p^T P_1 x_p + x_d^T P_2 x_d \tag{18}$$

with $P_1 = P_1^T > 0$ and $P_2 = P_2^T > 0$, then a simpler version of Theorem 1 is derived as follows, without proof (which does not need the Projection Lemma and is similar to that in [23]):

Corollary 1 *The $\mathcal{L}_2$ gain from d to y_d is less than γ_d if the following LMI is satisfied*

$$\begin{bmatrix} M_{11} & 0 & B_pEU - L^T & 0 & L^T D_p^T + Q_1 C_p^T \\ * & M_{22} & Q_2 C_d^T & B_d & 0 \\ * & * & -EU - UE^T & D_d & UE^T D_p^T \\ * & * & * & -\gamma_d I & 0 \\ * & * & * & * & -\gamma_d I_{n_y} \end{bmatrix} < 0 \tag{19}$$

with $Q_1 > 0$, $Q_2 > 0$ and

$$M_{11} = A_pQ_1 + Q_1A_p^T + B_pL + L^TB_p^T$$
$$M_{22} = A_dQ_2 + Q_2A_d^T$$

Here $U = W^{-1}$, $\gamma_d > 0$ and $L = FQ_1$.

Remark 5 Compared with the approach developed in Theorem 1, Corollary 1 provides a much simpler approach for implementation: 1) the algebraic loop can be resolved directly by setting $E = I$, since the gain for the LMI-optimization process in Corollary 1 is independent of E due to the existence of variable U; 2) the two step AW compensator construction procedure is avoided, since the Projection lemma is not used. However, the approach from Theorem 1 is less conservative than the one from Corollary 1, due to the different candidate Lyapunov functions employed. In Section 4, we discuss how to cope with the algebraic loops when $E \neq I$.

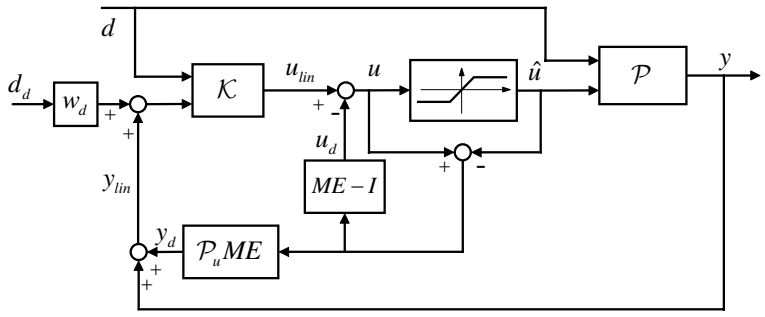

Figure 4: Anti-windup scheme modified from Fig. 1

3.2 Disturbance rejection AW (DRAW) with guaranteed robust performance

We consider the case where an additive uncertainty of the plant is incorporated into the AW-compensator synthesis. This result parallels that of [23], but introduces a novel approach to the argument on robustness for AW-compensator design, which particularly suits disturbance rejection problems. In general it is not possible to assume that a plant is modelled accurately, so that the consideration of model uncertainty is desirable.

We modify the approach in section 3.1 by augmenting d so that $\tilde{d} = \begin{bmatrix} d \\ d_d \end{bmatrix}$, where d_d has the same dimension as the plant output y, and d is the DSS testing signal. We replace $\mathcal{K}_w$ by $\begin{bmatrix} \mathcal{K}_w & w_d \mathcal{K}_y \end{bmatrix}$ and $\mathcal{P}_w$ by $\begin{bmatrix} \mathcal{P}_w & 0 \end{bmatrix}$, where the scalar $w_d > 0$. In this case, we have

$$\begin{aligned} \mathcal{P}_{\tilde{d}} &= (I - \mathcal{K}_y \mathcal{P}_u)^{-1} \left(\begin{bmatrix} \mathcal{K}_w & w_d \mathcal{K}_y \end{bmatrix} + \mathcal{K}_y \begin{bmatrix} \mathcal{P}_w & 0 \end{bmatrix} \right) \\ &\sim (A_{\tilde{d}}, B_{\tilde{d}}, C_{\tilde{d}}, D_{\tilde{d}}) \end{aligned} \tag{20}$$

Here we minimize not only the induced $\mathcal{L}_2$ gain $\|\mathcal{T}_{y_d}\|_\infty$, where $\mathcal{T}_{y_d} : \tilde{d} \mapsto y_d$, but also the $\mathcal{L}_2$ gain $\|\mathcal{T}_u\|_\infty$, where $\mathcal{T}_u : \tilde{d} \mapsto u$, in order to achieve a compromise between robustness and performance with respect to disturbance rejection. A minimal $\|\mathcal{T}_u\|_\infty$ guarantees robustness to additive uncertainty, while a small $\|\mathcal{T}_{y_d}\|_\infty$ guarantees the performance. It is more obvious to see this from Fig. 4, which is modified from Fig. 1.

From the above analysis, we have the following theorem:

Theorem 2 (Disturbance rejection AW (DRAW) with guaranteed robust performance)

Consider the $\mathcal{L}_2$ gain condition

$$\frac{1}{\gamma_d}\left\| \begin{array}{c} W_y^{\frac{1}{2}} y_d \\ W_r^{\frac{1}{2}} u \end{array} \right\|^2 - \gamma_d \|\tilde{d}\|^2 \leq 0 \tag{21}$$

where W_y and W_r are chosen diagonal weighting matrices during design to achieve a tradeoff between the minimization of $\mathcal{T}_{y_d} : \tilde{d} \mapsto y_d$ and $\mathcal{T}_u : \tilde{d} \mapsto u$. (21) is satisfied if there exists a symmetric positive definite matrix

$$P := \begin{bmatrix} P_{11} & P_{12} \\ P_{12}^T & P_{22} \end{bmatrix} \in \mathbb{R}^{n_p+n_d} \tag{22}$$

such that the following two linear matrix inequalities (LMIs) are satisfied

$$\begin{bmatrix} PA_o + A_o^T P + PW_A + W_A^T P & W_C + PW_B \\ W_C^T + W_B^T P & W_D \end{bmatrix} < 0 \tag{23}$$

with $A_o = \begin{bmatrix} A_p & 0 \\ 0 & A_{\tilde{d}} \end{bmatrix}$,

$$W_A = \begin{bmatrix} 0_{n_p} & B_p C_{\tilde{d}} \\ 0_{n_d \times n_p} & 0_{n_d} \end{bmatrix}$$

$$W_B = \begin{bmatrix} B_p D_{\tilde{d}} & 0_{n_p \times n_y} & -B_p \\ B_{\tilde{d}} & 0_{n_d \times n_y} & 0_{n_d, n_u} \end{bmatrix}$$

$$W_C = \begin{bmatrix} 0_{n_p \times n_w} & C_p^T & 0 \\ 0_{n_d \times n_w} & C_{\tilde{d}}^T D_p^T & 0 \end{bmatrix}$$

$$W_D = \begin{bmatrix} -\gamma_d I_{n_w} & D_{\tilde{d}}^T D_p^T & 0 \\ D_p D_{\tilde{d}} & -\gamma_d I_{n_y} W_y^{-1} & -D_p \\ 0 & -D_p^T & -\Gamma \end{bmatrix}$$

and

$$\begin{bmatrix} A_{\tilde{d}}^T P_{22} + P_{22} A_{\tilde{d}} & P_{22} B_{\tilde{d}} & C_{\tilde{d}}^T \\ B_{\tilde{d}}^T P_{22} & -\gamma_d I_{n_w} & D_{\tilde{d}}^T \\ C_{\tilde{d}} & D_d & -\gamma_d W_r^{-1} \end{bmatrix} < 0 \tag{24}$$

with $\gamma_d > 0$ and diagonal matrix $\Gamma = \mathrm{diag}(\gamma_1, \ldots, \gamma_{n_u}) > 0$.

Proof The proof is similar to that of Theorem 1. The diagonal matrix variable is derived from $\Gamma := \gamma_d W_r^{-1} W^2 + 2W \geq 0$ where the diagonal matrix $W > 0$ corresponds to the multiplier of the sector bound condition satisfied by the deadzone in Fig. 2. For a feasible solution Γ^*, it can be guaranteed that there is also a feasible solution W^*, as shown below. Since the diagonal matrices W_r and W are positive definite and γ_d is positive, Γ must be diagonal and positive definite. Hence we have

$$a w_i^2 + 2w_i - \gamma_i = 0 \quad \text{with } i = 1, ..., n_u$$

where $a := \gamma_d / w_{ri} > 0$, and w_i, γ_i, w_{ri} are diagonal elements of W, Γ and W_r. The solutions of w_i are

$$w_i = \frac{-2 \pm \sqrt{4 + a\gamma_i}}{2a}$$

so that there must be one solution greater than zero. □

Remark 6 An AW compensator can be constructed using the similar procedure as stated in Remark 3 for Theorem 1.

Remark 7 Define the operators $\mathcal{T}_{\hat{u}} : \tilde{d} \mapsto \hat{u}$, $\mathcal{T}_{\text{sat}} : u \mapsto \hat{u}$ in Fig. 1. We have $\|\mathcal{T}_{\hat{u}}\|_{i,2} = \|\mathcal{T}_{\text{sat}} \mathcal{T}_u\|_{i,2} \leq \|\mathcal{T}_{\text{sat}}\|_{i,2} \|\mathcal{T}_u\|_\infty = \|\mathcal{T}_u\|_\infty$, since $\|\mathcal{T}_{\text{sat}}\|_{i,2} = 1$. This means that the minimization of $\|\mathcal{T}_u\|_\infty$ implies the minimization of $\|\mathcal{T}_{\hat{u}}\|_{i,2}$, which contributes to the reduction of the $\mathcal{L}_2$ gains of the loops from $\tilde{d}$ to y_d and from d to $\hat{u}$. Note that the minimization of the operator from d to $\hat{u}$ is similar to a $\|KS\|_\infty$ minimization in robust control, where K is the robust controller and S is the closed-loop sensitivity [17]. Hence we remark that the inclusion of the minimization of $\|\mathcal{T}_u\|_\infty$ also minimizes $\|\mathcal{T}_{\hat{u}}\|_{i,2}$, ensuring robustness to additive plant uncertainty; that is, Theorem 2 poses a robust performance design approach. This follows by observation of Figs. 1 and 4 and the fact that we minimize the gain of the operator $d_d \mapsto \hat{u}$ when minimizing $\|\mathcal{T}_u\|_\infty$.

Remark 8 The $\mathcal{L}_2$ gain minimization of the mapping $\mathcal{T}_u$ reduces the input u to the nonlinear saturation operator, and hence it directly prevents saturation.

Remark 9 From Fig. 2, we can see that $\|\mathcal{T}_u\|_\infty \geq \|\mathcal{P}_d\|_\infty$. In particular, when $M = I$ and $E = I$, then we have $\|\mathcal{T}_u\|_\infty = \|\mathcal{P}_d\|_\infty$. This is the internal model control (IMC) AW

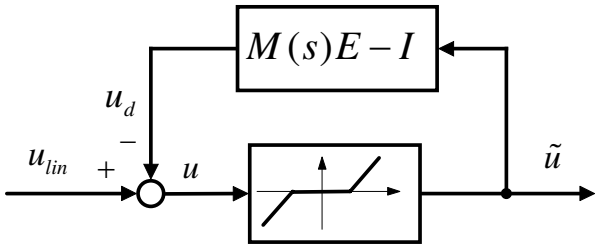

Figure 5: Algebraic loop in anti-windup compensation

case, which shows that the IMC AW is optimally robust. This is an important parallel to [23], where the AW approach is shown to be optimally robust for the IMC AW, although the approach to the design of a robust AW compensator is different from the approach in this paper.

Remark 10 For the DRAW approach of Theorem 2, a filter W_{fd} can also be included to modify $\mathcal{P}_d$, as $\mathcal{K}_{w_{new}} := \mathcal{K}_w W_{fd}$ and $\mathcal{P}_{w_{new}} := \mathcal{P}_w W_{fd}$. A proper choice of W_{fd} can further improve the performance.

4 Resolving algebraic loops

Although the scheme suggested in Theorem 1 in Section 3 can provide superior performance, one of the significant problems for implementation is the issue of algebraic loops, due to the matrix $E \neq I$. For AW-compensator implementation, it is necessary to explicitly compute the signals in the partial AW-structure of Fig. 5.

Some issues of algebraic loops, such as well-posedness, robust stability and solution method, have been investigated in, e.g. [10, 20, 21]. In [21], it is shown that an algebraic loop can be represented by a quadratic program; then the solution of the algebraic loop can be derived by resolving the quadratic program iteratively. A proposal for resolving scalar algebraic loops has been given in [4]. It was shown that the scalar algebraic loop is easily solved explicitly, rather than through implicit numerical algorithms, assuming that a saturation nonlinearity limits the control signal. This idea can be extended to algebraic loops with multiple signals.

The algebraic loop of Fig. 5 can be decomposed as in Fig. 6 so that we obtain a

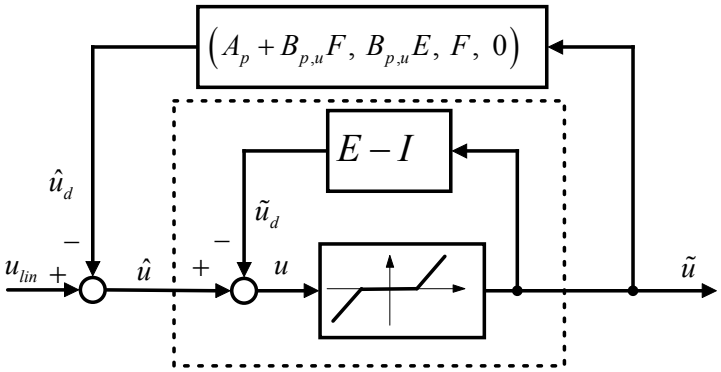

Figure 6: Equivalent two-loop representation of the algebraic loop

purely static operator $\hat{u} \mapsto \tilde{u}$ containing the algebraic loop, while an outer loop contains the dynamics of the system which do not contribute to the algebraic loop problem. Hence, to resolve the algebraic loop problem, it is sufficient that the static operator $\hat{u} \mapsto \tilde{u}$ is investigated. The following Lemmas will establish an approach to resolve the algebraic loop issue through explicit computation:

Lemma 1 *Assume that the deadzone limits are given by* $\bar{u} = [\bar{u}_1, \bar{u}_2, \cdots, \bar{u}_m]^T$*, E is invertible and* $\tilde{u}_i \neq 0$*,* $\forall\ i = 1, ..., m$*, then*

$$E^{-1}(\hat{u} - \mathrm{Sign}(u)\bar{u}) = \tilde{u} \tag{25}$$

Proof Given $\tilde{u}_i \neq 0$, $\tilde{u} + \mathrm{Sign}(u)\bar{u} = u$. Moreover, $u = \hat{u} - (E - I)\tilde{u}$. Hence, the assertion follows. □

This implies that, for scalar algebraic loops, an explicit solution is possible [4]:

Corollary 2 *Assuming the algebraic loop is scalar, i.e.* $E = e$ *and* $\mathrm{sign}(\hat{u}) = \mathrm{sign}(u)$*, then* $\frac{\mathrm{dz}(\hat{u})}{e} = \tilde{u}$*.*

Thus, the scalar algebraic loop has a simple explicit solution.

For multi-variable algebraic loops, it would be desirable to exploit the relationship in (25). Hence, we wish to compute $\tilde{u}$ for a given $\hat{u}$. However, this is only possible with equation (25) if we have knowledge of $\mathrm{Sign}(u)$. The following Lemma establishes the necessary condition:

Lemma 2 *Assume that the deadzone limits are given by* $\bar{u} = [\bar{u}_1, \bar{u}_2, \cdots, \bar{u}_m]^T$, *$E$ is invertible and* $\tilde{u}_i \neq 0$, $\forall\ i = 1, ..., m$. *Then* $\mathrm{Sign}(E^{-1}\hat{u}) = \mathrm{Sign}(\tilde{u}) = \mathrm{Sign}(u)$ *if, for any diagonal matrix* $\mathcal{D} = diag\,(d_1, d_2, \cdots, d_m)$ *satisfying* $|d_i| = 1$, $d_i \in \mathbb{R}$, *the following holds:*

$$\mathrm{Sign}(E^{-1}\mathcal{D}\bar{u}) = \mathcal{D} \tag{26}$$

Proof It has been established using (25) that $E^{-1}\hat{u} = \tilde{u} + E^{-1}\,\mathrm{Sign}(u)\bar{u}$. Moreover, $\mathrm{Sign}(u) = \mathrm{Sign}(\tilde{u})$. Hence, $E^{-1}\hat{u} = \tilde{u} + E^{-1}\,\mathrm{Sign}(\tilde{u})\bar{u}$ and $\mathrm{Sign}(E^{-1}\,\mathrm{Sign}(\tilde{u})\bar{u}) = \mathrm{Sign}(\tilde{u})$. Thus, the assertion follows. □

Equation (26) is satisfied if and only if the matrix $(E^{-1}\,\mathrm{diag}(\bar{u}))$ is strictly diagonally dominant. The following Corollary is necessary for resolving an algebraic loop and is a generalization of Corollary 2 of [4].

Corollary 3 *Assume that the conditions of Lemma 1 hold and* $(E^{-1}\,\mathrm{diag}(\bar{u}))$ *is strictly diagonally dominant, then* $E^{-1}(\hat{u} - \mathrm{Sign}(E^{-1}\hat{u})\bar{u}) = \tilde{u}$.

Note that the LMIs of (13) and (19) guarantee that the algebraic loop has a solution which is unique [24]. Hence, it is now possible to resolve an algebraic loop for a strictly diagonally dominant matrix $(E^{-1}\,\mathrm{diag}(\bar{u}))$. As an example, an algebraic loop with two constrained signals, $m = 2$, shall suffice:

$$E = \begin{bmatrix} e_{11} & e_{12} \\ e_{21} & e_{22} \end{bmatrix}$$

The following steps are to be taken for given $\hat{u} = [\hat{u}_1\ \hat{u}_2]^T$:

1. Compute $\tilde{u} = E^{-1}(\hat{u} - \mathrm{Sign}(E^{-1}\hat{u})\bar{u})$, $\tilde{u} = [\tilde{u}_1\ \tilde{u}_2]^T$. If $\tilde{u}_1 \neq 0$, $\tilde{u}_2 \neq 0$ and $\mathrm{Sign}(E^{-1}\hat{u}) = \mathrm{Sign}(\tilde{u})$, then a solution of the algebraic loop is found.

   Otherwise, go to step 2):

2. Assume $\tilde{u}_1 = 0$. This is satisfied if $\mathrm{dz}_1(\hat{u}_1 - e_{12}\tilde{u}_2) = 0$ for $\tilde{u}_2 = \mathrm{dz}_2(\hat{u}_2)/e_{22}$.

   Otherwise, go to step 3):

3. Assume $\tilde{u}_2 = 0$. This is satisfied if $\mathrm{dz}_2(\hat{u}_2 - e_{21}\tilde{u}_1) = 0$ for $\tilde{u}_1 = \mathrm{dz}_1(\hat{u}_1)/e_{11}$.

This procedure will guarantee the solution of the algebraic loop and can be extended to $m > 2$ in a straightforward manner.

5 Two other existing AW approaches

For completeness and for comparison, we also briefly present two other AW compensators designed by the robust AW approach in [23] and the IMC AW approach [29].

5.1 The robust AW (RAW) approach of [23]

In Figs. 1 and 2, if assuming $E = I$ and $M(\infty) = I$, then we have the framework used to develop the robust AW approach in [23]. This approach is to achieve a tradeoff between the performance and robustness, by minimizing the $\mathcal{L}_2$ gain:

$$\frac{1}{\gamma}\left\| \begin{array}{c} W_y^{\frac{1}{2}} y_d \\ W_r^{\frac{1}{2}} z_\Delta \end{array} \right\|^2 - \gamma \|u_{\text{lin}}\|^2 \leq 0 \tag{27}$$

which is composed of a weighted combination of two mappings $\mathcal{T}_p : u_{\text{lin}} \mapsto y_d$ representing the performance and $\mathcal{T}_r : u_{\text{lin}} \mapsto z_\Delta$ representing the robust stability, with W_y and W_r as the corresponding weights. This approach leads to the LMI (23) in [23]:

$$\begin{bmatrix} M_{11} & M_{12} & 0 & M_{14} & L^T \\ \star & -2U & I_{n_u} & UD_p^T & U \\ \star & \star & -\gamma I_{n_u} & 0 & -I \\ \star & \star & \star & -\gamma W_y^{-1} & 0 \\ \star & \star & \star & \star & -\gamma W_r^{-1} \end{bmatrix} < 0 \tag{28}$$

with $M_{11} = A_pQ + QA_p^T + B_pL + L^TB_p^T$, $M_{12} = B_pU - L^T$, $M_{14} = QC_p^T + L^TD_p^T$, $Q = Q^T > 0$, $L = FQ$, diagonal matrix $U > 0$ and scalar $\gamma > 0$. A beneficial by-product of involving the extra map $\mathcal{T}_r$ in the minimization is the removal of fast poles of the compensator.

5.2 IMC AW approach [29]

It is noted that the IMC AW in [29] is subsumed within the AW framework of [23] when we set $M = I$ and $E = I$ in Fig. 1.

6 AW designs for DSS systems

The principal idea of substructuring is to test the critical subcomponents of a large engineering system (represented as a physical substructure), while the remainder is simultaneously represented as a real-time numerical model (called the numerical substructure). Hence, a DSS consists of at least two components:

- a physical substructure which is to be tested practically, together with actuators (called the transfer system), which exert the necessary forces or torques on the physical test specimen itself.
- a numerical substructure, representing the dynamics of the remaining parts of the system.

The substructuring approach can be more advantageous than traditional testing methods, such as full-size testing of the entire system, scale-model testing, pseudo-dynamic testing and purely numerical testing [27]. An important issue of the substructuring method is the need for close synchronization of the physical and numerical substructures. This demands a high fidelity of control to synchronize the signals at the interface between the two substructures. However, the uncertainties and the nonlinearities associated with the dynamical interaction between the two substructures, together with the dynamics of the transfer system, will normally cause problems with synchronization. One of these problems is associated with the actuator saturation, which may degrade the DSS performance. Model Predictive Control (MPC) and AW compensation are two possible control strategies appropriate for actuator saturation problems. The real-time implementation of MPC on DSS has been performed on a hydraulically-actuated test of a quasi-motorcycle system in [14]. However, the on-line implementation of MPC on a fast system may have problems, due to the computation time required for solving the optimization problem at each sampling time. In this case, the AW compensation can be used as an alternative approach to cope with the actuator saturation problem in DSS.

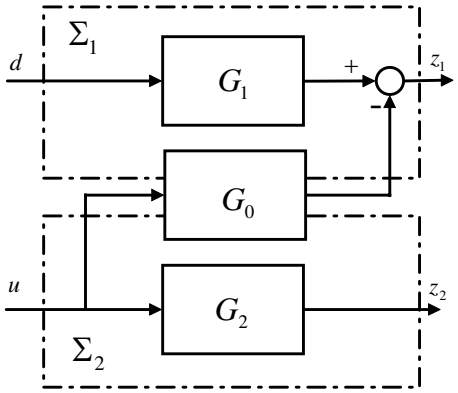

Figure 7: The substructured system [18]

To facilitate the DSS controller design, a general DSS framework was proposed in [18] (see Fig. 7), where

$$z_1 = G_1 d - G_0 u \tag{29}$$

$$z_2 = G_2 u \tag{30}$$

Here, z_1 and z_2 are the interface signals from the physical and numerical substructures, which are to be synchronized; d is the testing, or external excitation, signal; u is the control signal provided by a DSS controller; G_1 and G_2 represent the dynamics of the numerical and physical substructures, and G_0 is the interaction dynamics between the two substructures. We use the generalized set $\{\Sigma_1, \Sigma_2\}$ to represent the numerical and physical substructures $\{\Sigma_N, \Sigma_P\}$ or, conversely, $\{\Sigma_P, \Sigma_N\}$. For more details about the substructuring problem, see [18] and the references therein. The control objective is to use a synchronizing control signal u to make the output z_2 of Σ_2 track the output z_1 of Σ_1, subject to the excitation signal, d. The smaller the tracking error, $e = z_1 - z_2$, the closer the DSS is to the real system. If the excitation signal, d, is assumed to be a measured disturbance, then the synchronization of DSS can be viewed as a regulation control problem with measured disturbance attenuation. The DSS shown in Fig. 7 can be cast into the AW framework in this paper by setting $\mathcal{P}_u = -(G_0 + G_2)$ and $\mathcal{P}_w = G_1$.

In the following, we introduce two DSS examples and use the numerical simulation results to demonstrate the efficacy of using AW compensation techniques, and to provide a comparison of the AW approaches presented in this paper.

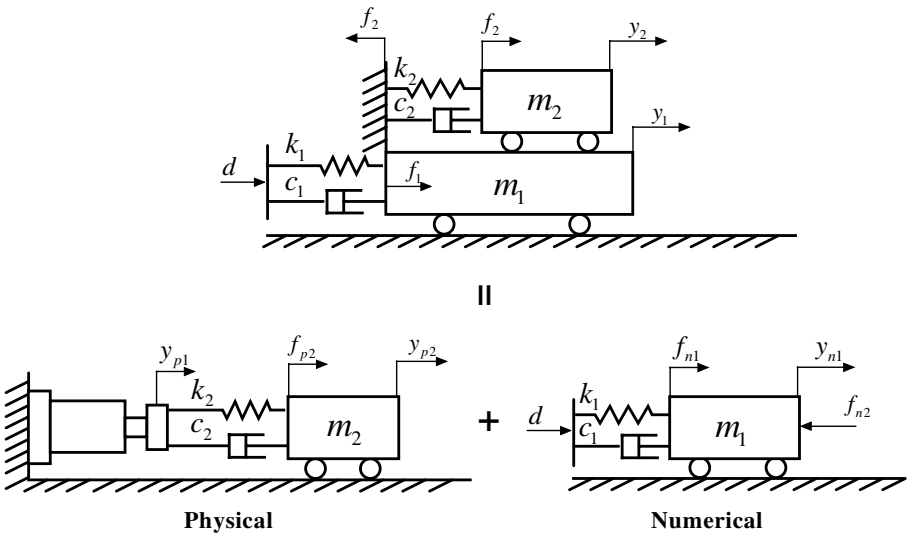

Figure 8: The DSS formulation of the mass damper system

6.1 Mass-damper system

In this example, we consider the seismic response reduction problem of a model building with a tuned mass-damper. This system is used for small-scale demonstration purposes. A small-scale shaking table test rig is used to establish a DSS system: the shaking table, acting as the mass-damper, is assumed to be the physical substructure, while the building is assumed to be the numerical substructure. The testing signal simulates the horizontal ground vibration during an earthquake, which can excite the fundamental mode of vibration of a tall building in the 1 Hz region. The DSS control aims to synchronize the two substructures so that the response of the DSS is as close as possible to that of the emulated system, subject to the same excitation signal.

6.1.1 The mass-damper DSS

A building with a damper system can be illustrated as in Fig. 8, where the top mass m_2 with damper c_2 and spring k_2 represents the damper system (physical substructure), and the bottom mass m_1 with damper c_1 and spring k_1 represents the building (the numerical

substructure), so that:

$$m_1\ddot{y}_{n1} = f_{n1} - f_{n2} \tag{31}$$

$$m_2\ddot{y}_{p2} = f_{p2} \tag{32}$$

$$f_{n1} = k_1(d - y_{n1}) + c_1(\dot{d} - \dot{y}_{n1}) \tag{33}$$

$$f_{p2} = k_2(y_{p1} - y_{p2}) + c_2(\dot{y}_{p1} - \dot{y}_{p2}) \tag{34}$$

where we use the subscripts n and p to represent the variables associated with the numerical and physical substructures, respectively. We assume that the interaction force is the constraint variable, i.e. $f_{p2} = f_{n2}$, and the objective is to minimize the physical substructure displacement output y_{p1}, generated by an actuator, with the numerical substructure displacement output y_{n1}. We define the DSS error as $e := y_{n1} - y_{p1}$. Hence, after some manipulation, the DSS is given by:

$$y_{n1} = G_d d - G_y y_{p1} \tag{35}$$

$$y_{p1} = G_a u \tag{36}$$

where $G_a = \frac{b}{s+a}$ is the transfer function for the transfer system actuator, and

$$G_d = \frac{c_1 s + k_1}{m_1 s^2 + c_1 s + k_1}$$

$$G_y = \frac{m_2 s^2 (c_2 s + k_2)}{(m_1 s^2 + c_1 s + k_1)(m_2 s^2 + c_2 s + k_2)}$$

Then the DSS error is

$$e = G_d d - (G_y + 1) G_a u = G_d d + G_u u \tag{37}$$

with $G_u = -(G_y + 1)G_a$.

The parameters are chosen as $m_1 = 150kg$, $k_1 = 7708.7$ N/m, $c_1 = 100$ Ns/m, $m_2 = 7.8kg$, $k_2 = 400$ N/m, $c_2 = 14.65$ Ns/m, $a = 8\text{s}^{-1}$ and $b = 0.3$ mV/s. This choice of parameters lead to the fundamental mode natural frequency of the building given by $\sqrt{k_1/m_1} \approx 7.17$ rad/s.

6.1.2 Designs of controller and AW compensators

We calculate a linear feedback controller K_e so that the loop shape $L = G_u K_e$ optimally matches a target loop shape of G_t, using the MATLAB$^{\text{TM}}$ routine `Ke=loopsyn(Gu, Gt)`.

We also choose $G_t = \frac{25}{s}$, which has a crossover frequency of 25 rad/s. The resulting feedback controller has a guaranteed infinite gain margin and a phase margin of 90 degrees. The complementary sensitivity response $25/(s+25)$ provides a -20 dB/dec roll-off above 25 rad/s, creating robustness to relative plant output uncertainty in a small gain sense. Hence, this guarantees a sufficiently robust controller to cope with the model mismatch from either parametric uncertainty or unmodelled dynamics. The feedforward controller is determined by an inverse controller $K_d = G_u^{-1}G_d$. Here we use the nominal values of the actuators to calculate the controllers and assume the actuator in the plant has the parameters $a = 10$ s^{-1}, $b = 0.8$ mV/s, so that a model mismatch exists. The simulations were performed in four cases: the linear controller alone, the linear controller plus the IMC anti-windup (IMC AW), the linear controller plus the robust anti-windup (RAW) and the linear controller plus the robust disturbance rejection anti-windup (DRAW). For the purpose of illustration, we set the actuator's input constraint as $-0.2 \sim 0.2$ V, corresponding to an output constraint of $-0.016 \sim 0.016$ m. The testing signal was a chirp signal sweeping from 0.2 Hz to 3 Hz, with a magnitude of 0.01 m and a time duration of 20 s. In the design of the RAW compensator the weights were chosen as $W_p = 1$ and $W_r = 0.007$; while in the design of the DRAW compensator, the weights were chosen as $W_p = 1$ and $W_u = 0.007$. We also chose a disturbance filter $W_{fd} = \frac{0.5(s+600)}{s+1.2}$, to penalize the testing signal under 3 Hz in the design of the DRAW.

6.1.3 Simulation results

The DSS errors and the actuator inputs for the cases when using the linear controller alone and the case when using DRAW compensator are shown in Figs. 9 and 10, which demonstrate the performance improvement of the DRAW over the linear controller alone, while the input remains strictly within $-0.2 \sim 0.2$ V. We plot the integral squared errors of the DSS errors, as shown in Fig. 11, which shows that the AW compensators can improve the performances over the linear controller alone. The performances of the AW compensators with respect to the DSS error reduction are in the order DRAW>RAW>IMC AW. To make a better comparison of the performances when the actuator is subject to different magnitude limits, we compare the ISE final values in Table 1, which also confirm the

Table 1: A comparison of ISE final values at different actuator limits

Saturation Limit (V)	±0.15	±0.2	±0.25
Without AW	0.1877	0.1681	0.1444
IMC AW	0.1594	0.1388	0.1201
RAW	0.1532	0.1323	0.1138
DRAW	0.1319	0.1138	0.0986

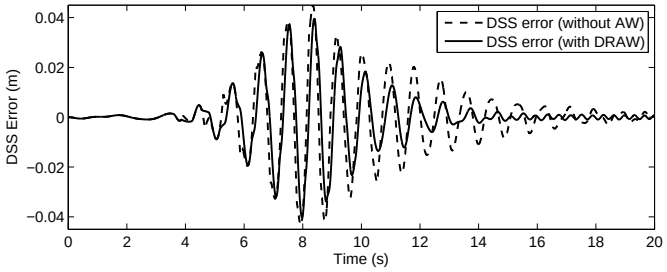

Figure 9: The DSS errors (without an AW compensator and with a DRAW compensator)

same conclusion as the ISE plot. Moreover, it is coincident that the ISE final value of DRAW in the case of saturation (±0.25 V) is the same with that of RAW in the case of saturation (±0.2 V).

6.2 A quasi-motorcycle suspension system

We now consider the simulation of a quasi-motorcycle system.

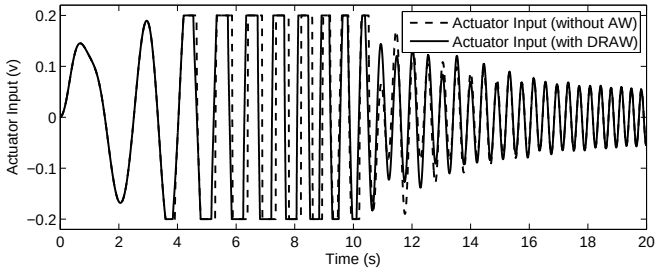

Figure 10: The actuator inputs (without an AW compensator and with a DRAW compensator)

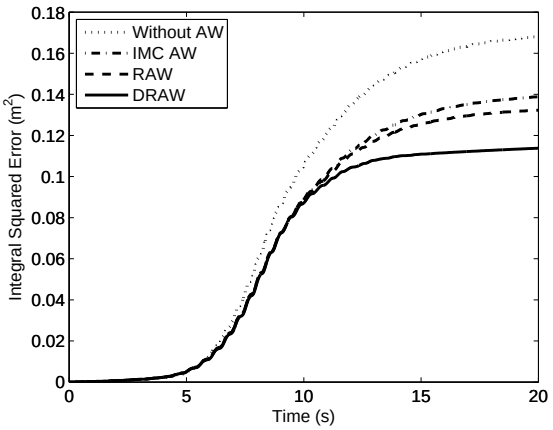

Figure 11: A comparison of the ISE plots of the DSS errors

6.2.1 The DSS of the quasi-motorcycle suspension system

In this case study, we separate the system into the following parts: the quasi-motorcycle body with two suspension struts, and the front and rear wheels/tyres modelled numerically, as shown in Fig. 12. We call this a *single mode* substructure. We can also model one wheel/tyre numerically and the other physically, or two wheels/tyres physically and the body with two suspension struts numerically, depending on the problems that we are interested in. The control objective is to synchronize the physical and numerical substructures by minimizing the displacement errors $\{y_1, y_2\}$ between the front/rear suspension struts $\{y_{a31}, y_{a32}\}$ and front/rear wheel hubs $\{y_{31}, y_{32}\}$, subject to external testing signals $\{d_1, d_2\}$, (which can be viewed as road disturbances). The model for this system can be established and represented in the standard DSS framework, so that G_1 only contains the numerical substructure parameters, G_2 the substructure parameters of the physical components, i.e. the quasi-motor cycle. The interaction transfer function G_0 contains elements of both the numerical and physical substructures. See [19] for the details of the model development, the parameter values, and the LSC and MSC control designs. Here

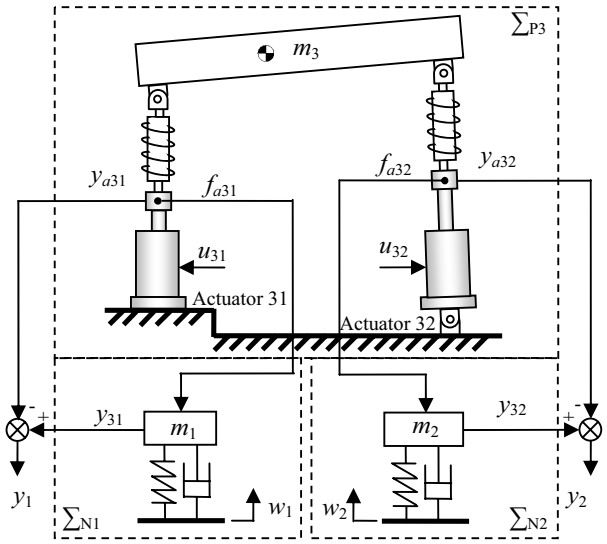

Figure 12: Substructuring for a motor cycle suspension

we only present the transfer function matrices for the DSS:

$$G_0 = \begin{bmatrix} G_{0(1,1)} & G_{0(1,2)} \\ G_{0(2,1)} & G_{0(2,2)} \end{bmatrix} \qquad G_1 = \begin{bmatrix} G_{1(1,1)} & 0 \\ 0 & G_{1(2,2)} \end{bmatrix}$$

$$G_2 = \begin{bmatrix} \frac{8.3}{s+8.3} & 0 \\ 0 & \frac{8.3}{s+8.3} \end{bmatrix}$$

with

$$G_{0(1,1)} = G_{0(2,2)} = \frac{413.4s^3 + 2953s^2}{s^5 + 52.57s^4 + 1358s^3 + 1.778e4s^2 + 1.26e5s + 3.873e5}$$

$$G_{0(1,2)} = G_{0(2,1)} = \frac{206.3s^3 + 1474s^2}{s^5 + 52.57s^4 + 1358s^3 + 1.778e4s^2 + 1.26e5s + 3.873e5}$$

$$G_{1(1,1)} = G_{1(2,2)} = \frac{30.27s + 466.7}{s^2 + 30.27s + 466.7}$$

Note that the above models are used for the designs of the controller and AW compensators, and are established via the linearizing approximations: $\sin\theta \approx \theta$ and $\cos\theta \approx 1$. However, the full nonlinear dynamics are modelled in SIMULINK$^{\text{TM}}$, for the purpose of simulation. See [19] for the details of the model development.

In the following, we first design an LQG controller for the system ignoring the actuator limits, then design AW compensators respectively based on Theorem 1, Corollary 1 and the original W&P approach (Lemma 1).

6.2.2 The designs of the LQG controller and AW compensators

Suppose that the transfer functions $G_0(s)$, $G_1(s)$ and $G_2(s)$ are strictly proper and their state space matrices are $G_i(s) \sim (A_i, B_i, C_i, 0)$ with $i = 0, 1, 2$. Then, the state space realization for the whole system can be written as

$$\dot{x} = Ax + B_u u + B_d d \tag{38a}$$

$$y = Cx \tag{38b}$$

with $x = \begin{bmatrix} x_0^T & x_1^T & x_2^T \end{bmatrix}^T \in \mathbb{R}^{n_x}$, $y \in \mathbb{R}^{n_u}$ and

$$A = \begin{bmatrix} A_0 & 0 & 0 \\ 0 & A_1 & 0 \\ 0 & 0 & A_2 \end{bmatrix} \qquad B_u = \begin{bmatrix} B_0 \\ 0 \\ B_2 \end{bmatrix} \qquad B_d = \begin{bmatrix} 0 \\ B_1 \\ 0 \end{bmatrix}$$

$$C = \begin{bmatrix} -C_0 & C_1 & -C_2 \end{bmatrix}$$

The corresponding equations for a linear observer are

$$\dot{\hat{x}} = A\hat{x} + B_u u + B_d d + L(y - \hat{y}) \tag{39a}$$

$$\hat{y} = C\hat{x} \tag{39b}$$

Suppose the feedback gain K is computed from the algebraic Ricatti equation so that

$$u = -K\hat{x} \tag{40}$$

Substituting (40) and (39b) into (39a) leads to the LQG controller-observer equations:

$$\dot{\hat{x}} = (A - LC - B_u K)\hat{x} + B_d d + Ly \tag{41a}$$

$$u = -K\hat{x} \tag{41b}$$

Therefore,

$$A_c = A - LC - B_u K \qquad B_{c,d} = B_d \qquad B_{c,y} = L$$

$$C_c = -K \qquad D_{c,d} = 0 \qquad D_{c,y} = 0$$

The weights of the Kalman filter when designing the observer are chosen as $Q_n = 10^5 I_{n_y}$ and $R_n = I_{n_u}$; the weights for the algebraic Ricatti equation are $Q = 5 \times 10^3 \times C_p^T C_p$

and $R = I_{n_u}$. We use a pulse signal with amplitude 0.01m, period 2s and pulse width 0.2s as the testing signal. The limits for both actuators are $[-0.012, 0.012]$m.

Based on the LQG controller, we make a comparison of four cases: (a) without AW compensator; (b) with AW compensator – minimizing the $\mathcal{L}_2$ gain from u_{lin} to y_d (Lemma 1); (c) with AW compensator – minimizing the $\mathcal{L}_2$ gain from d to y_d (Corollary 1); and (d) with AW compensator – minimizing the $\mathcal{L}_2$ gain from d to y_d (Theorem 1);

For case (b), the $\mathcal{L}_2$ gain from u_{lin} to y_d is $\gamma_u = 1.3903$.

For case (c), if set $E = I_{n_u}$, then the $\mathcal{L}_2$ gain from d to y_d is $\gamma_d = 4.2565$.

For case (d), the $\mathcal{L}_2$ gain from d to y_d and the variable E (see Remark 3) are

$$\gamma_d = 1.2761 \qquad\qquad E = \begin{bmatrix} 4.5424 & -0.4778 \\ -0.4779 & 4.5426 \end{bmatrix}$$

Here, $E^{-1}\,\text{diag}(0.012, 0.012)$ is strictly diagonally dominant, hence the algebraic loop can be resolved using the approach in Section 4 (see Corollary 3).

From the results, we note that the $\mathcal{L}_2$ gain γ_d is greatly reduced when using the approach based on Theorem 1, compared with the one based on Corollary 1.

6.2.3 Simulation results

Fig. 13 shows the interaction interface errors of the DSS for 4 cases. We can see that the performance in case (d) is better than other three cases, while the performance in cases (b) and (c) is not better than in (a). This shows that the original W&P approach is not suitable for the disturbance rejection problem in this example and the approach based on Theorem 1 is much less conservative than the one based on Corollary 1. Fig. 14 shows the control inputs of the plant in the four cases and we can see that the control input magnitude of case (d) is less than the ones of other three cases.

7 Conclusion

We have developed an approach to improve system performance for disturbance rejection problems based on the W&P scheme. The novel feature of this new approach is that a transfer function representing the effect of the disturbance on the nonlinear loop is

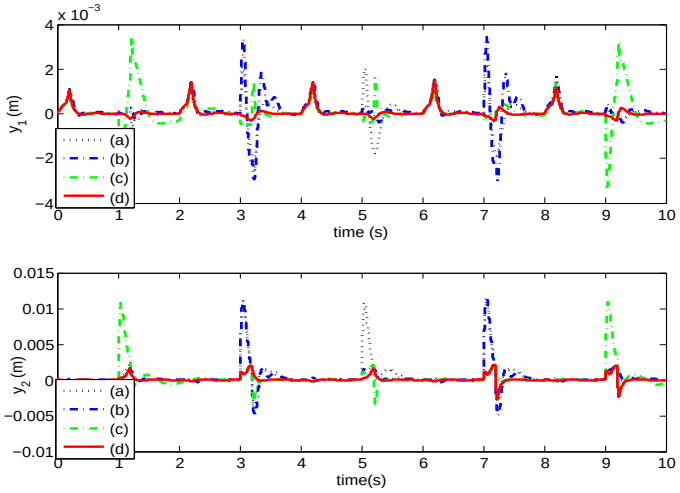

Figure 13: Comparison of the DSS outputs of the four cases (a)∼(d).

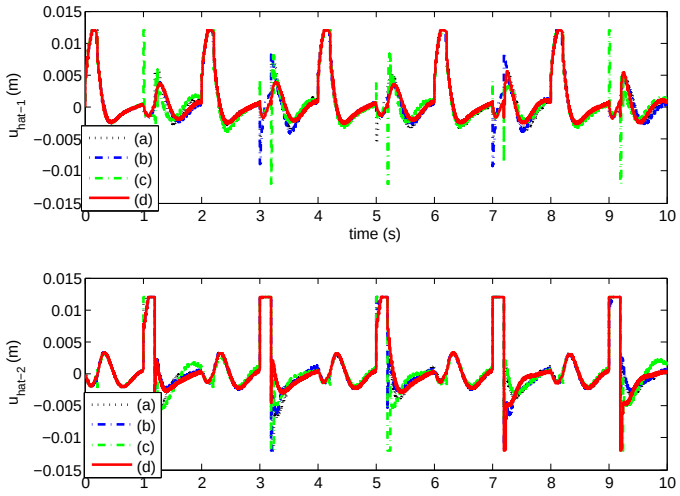

Figure 14: Comparison of the DSS control signals of the four cases (a)∼(d).

considered in the compensator synthesis. The algebraic loop problem associated with this AW-compensator is resolved by a generic approach. The additive uncertainty of the plant is incorporated into the AW-compensator synthesis for disturbance rejection problems. This approach is applied to DSS examples to cope with the actuator limits. The benefit of using this approach is also shown in two simulation examples.

A Proof of Theorem 1

Proof We choose a Lyapunov function candidate as

$$V = \xi^T P \xi \tag{42}$$

with $\xi := [x_p^T, x_d^T]^T$ and P as (9).

Define the following relations and matrices:

$$\begin{aligned} \tilde{A} &= A_o + H_1^T \Lambda G_1 & \tilde{B} &= B_o + H_1^T \Lambda G_2 \\ \tilde{C}_d &= C_{do} + H_2^T \Lambda G_1 & \tilde{D}_d &= D_{do} + H_2^T \Lambda G_2 \\ \tilde{C}_p &= C_{po} + H_3^T \Lambda G_1 & \tilde{D}_p &= H_3^T \Lambda G_2 \end{aligned} \tag{43}$$

with

$$\begin{aligned} B_o &= \begin{bmatrix} 0_{n_p \times n_u} & 0_{n_p \times n_w} \\ 0_{n_d \times n_u} & B_d \end{bmatrix} & C_{do} &= \begin{bmatrix} 0_{n_u \times n_p} & C_d \\ 0_{n_w \times n_p} & 0_{n_w \times n_d} \end{bmatrix} \\ D_{do} &= \begin{bmatrix} 0_{n_u} & D_d \\ 0_{n_w \times n_u} & 0_{n_w} \end{bmatrix} & C_{po} &= \begin{bmatrix} C_p & 0_{n_y \times n_d} \end{bmatrix} \\ G_1 &= \begin{bmatrix} I_{n_p} & 0_{n_p \times n_d} \\ 0_{n_u \times n_p} & 0_{n_u \times n_d} \end{bmatrix} & G_2 &= \begin{bmatrix} 0_{n_p \times n_u} & 0_{n_p \times n_w} \\ I_{n_u} & 0_{n_u \times n_w} \end{bmatrix} \\ H_1^T &= \begin{bmatrix} B_p \\ 0_{n_d \times n_u} \end{bmatrix} & H_2^T &= \begin{bmatrix} -I_{n_u} \\ 0_{n_w \times n_u} \end{bmatrix} \\ H_3^T &= D_p & \Lambda &= \begin{bmatrix} F & E \end{bmatrix} \end{aligned}$$

To guarantee the $\mathcal{L}_2$ gain performance, suppose $P = P^T > 0$ is determined so that

$$\frac{d}{dt}\xi^T P \xi + 2\tilde{u}^T W(u_{\text{lin}} - F x_p - E\tilde{u}) < \gamma_d \|d\|^2 - \frac{1}{\gamma_d}\|y_d\|^2 \tag{44}$$

which is derived from the S-procedure. Note that integrating both sides of (44) from 0 to ∞, we have

$$\begin{aligned} &V(\infty) - V(0) + 2\int_0^\infty \left(\tilde{u}^T W(u_{\text{lin}} - Fx_p - E\tilde{u})\right) dt \\ &< \int_0^\infty \left(\gamma_d \|d\|^2 - \frac{1}{\gamma_d}\|y_d\|^2\right) dt \end{aligned}$$

which implies that the $\mathcal{L}_2$ gain from d to y_d is less than γ_d.

Using Schur complements, (44) can be converted to

$$\begin{bmatrix} \tilde{A}^T P + P\tilde{A} & P\tilde{B} + \tilde{C}_d^T \tilde{W} & \tilde{C}_p^T \\ \tilde{B}^T P + \tilde{W}\tilde{C}_d & \tilde{W}\tilde{D}_d + \tilde{D}_d^T \tilde{W} - \gamma_d \tilde{I}_{n_w} & \tilde{D}_p^T \\ \tilde{C}_p & \tilde{D}_p & -\gamma_d I_{n_y} \end{bmatrix} < 0 \tag{45}$$

with $\tilde{W}$ as (17).

Define

$$Q = P^{-1} = \begin{bmatrix} Q_{11} & Q_{12} \\ Q_{12}^T & Q_{22} \end{bmatrix} \tag{46}$$

Substituting (43) into (45) leads to

$$\Psi + H^T \Lambda G + G^T \Lambda^T H < 0 \tag{47}$$

where Ψ is (14), G is (16) and

$$H = \underbrace{\left[\begin{array}{c|c|c} H_1 & H_2 & H_3 \end{array}\right]}_{H_O} \underbrace{\text{diag}(P, \tilde{W}, I)}_{\bar{T}} \tag{48}$$

with

$$H_O = \left[\begin{array}{cc|cc|c} B_p^T & 0_{n_u \times n_d} & -I_{n_u} & 0_{n_u \times n_w} & D_p^T \end{array}\right]$$

Using the projection lemma, the satisfaction of (13) is equivalent to the satisfaction of the two matrix inequalities

$$W_H^T \Psi W_H < 0 \qquad\qquad W_G^T \Psi W_G < 0$$

Here the columns of W_H span the null space of H such that $HW_H = 0$ and the columns of W_G span the null space of G such that $GW_G = 0$. Also, define the matrix W_{H_O} whose

columns span the null space of H_O, such that $H_O W_{H_O} = 0$

$$W_{H_O} = \left[\begin{array}{cc|cc|c} I_{n_p} & 0 & B_p & 0 & 0 \\ 0 & I_{n_d} & 0 & 0 & 0 \\ \hline 0 & 0 & 0 & I_{n_w} & 0 \\ 0 & 0 & D_p & 0 & I_{n_y} \end{array}\right]^T \tag{49}$$

Since $H_O W_{H_O} = H\bar{T}^{-1}\bar{T}W_H = 0$, we have $W_{H_o} = \bar{T}W_H$. Hence $W_H = \bar{T}^{-1}W_{H_o}$ and

$$\begin{aligned} W_H^T \Psi W_H &= W_{H_o}^T \underbrace{\bar{T}^{-1}\Psi\bar{T}^{-1}}_{\bar{\Psi}} W_{H_o} \\ &= \begin{bmatrix} A_o Q + Q A_o^T + W_A Q + Q W_A^T & Q W_C + W_B \\ W_C^T Q + W_B^T & W_D \end{bmatrix} < 0 \end{aligned} \tag{50}$$

Pre- and post-multiplying (50) by $\mathrm{diag}(P, I)$ results in (10).

Similarly,

$$W_G = \begin{bmatrix} 0 & I_{n_d} & 0 & 0 & 0 \\ 0 & 0 & 0 & I_{n_w} & 0 \\ 0 & 0 & 0 & 0 & I_{n_y} \end{bmatrix}^T \tag{51}$$

Substitution of W_G into $W_G^T \Psi W_G < 0$ results in

$$W_G^T \Psi W_G = \begin{bmatrix} A_d^T P_{22} + P_{22} A_d & P_{22} B_d & 0 \\ B_d^T P_{22} & -\gamma_d I_{n_w} & 0 \\ 0 & 0 & -\gamma_d I_{n_y} \end{bmatrix} < 0 \tag{52}$$

which is equivalent to (12). □

Acknowledgment

The authors gratefully acknowledge the support of the UK Engineering & Physical Sciences Research Council, grant number: EP/D036917, *Adaptive Control of Generalised Dynamically Substructured Systems*, in the pursuance of this work.

References

[1] F. Forni and S. Galeani. Gain-scheduled, model-based anti-windup for LPV systems. *Automatica*, 46(1):222 – 225, 2010.

[2] S. Galeani, S. Nicosia, A. R. Teel, and L. Zaccarian. Output feedback compensators for weakened anti-windup of additively perturbed systems. In *IFAC World Congress*, 2005.

[3] G. Grimm, J. Hatfield, I. Postlethwaite, A. R. Teel, M. C. Turner, and L. Zaccarian. Antiwindup for Stable Linear Systems With Input Saturation: An LMI-Based Synthesis. *IEEE Trans. on Automatic Control*, 48(9):1509–1525, 2003.

[4] G. Herrmann, B. Hredzak, M. C. Turner, I. Postlethwaite, and G. Guo. Improvement of a novel dual-stage large-span track-seeking and track-following method using anti-windup compensation. In *Proc. of the 2006 American Control Conference, Minneapolis, MN, USA*, 2006.

[5] G. Herrmann, B. Hredzak, M. C. Turner, I. Postlethwaite, and G. Guo. Discrete robust anti-windup to improve a novel dual-stage large-span track-seek/following method. *IEEE Transactions on Control Systems Technology*, 16(6):1342–1351, 2008.

[6] G. Herrmann, M. Turner, I. Postlethwaite, and G. Guo. Practical implementation of a novel anti-windup scheme in a HDD-dual-stage servo-system. *IEEE/ASME Transactions on Mechatronics*, 9(3):580–592, 2004.

[7] G. Herrmann, M. C. Turner, and I. Postlethwaite. Some new results on anti-windup-conditioning using the Weston-Postlethwaite approach. In *the 43rd IEEE Conference on Decision and Control*, pages 5047–5052, Atlantis, Paradise Island, Bahamas, 2004.

[8] R. A. Horn and C. R. Johnson. *Matrix Analysis*. Cambridge University Press, 1985.

[9] T. Hu, B. Huang, and Z. Lin. Absolute stability with a generalized sector condition. *IEEE Trans. on Automatic Control*, 9(4):535–548, 2004.

[10] T. Hu, A. R. Teel, and L. Zaccarian. Stability and performance for saturated systems via quadratic and nonquadratic Lyapunov functions. *IEEE Transactions on Automatic Control*, 51(11):1770 –1786, 2006.

[11] J. M. Gomes da Silva Jr. and S. Tarbouriech. Anti-windup design with guaranteed regions of stability: an LMI approach. *IEEE Trans. on Automatic Control*, 50(1):106–111, 2005.

[12] M. V. Kothare, P. J. Campo, M. Morari, and C. N. Nett. A unified framework for the study of anti-windup designs. *Automatica*, 30:1869–1883, 1994.

[13] G. Li, W. P. Heath, and B. Lennox. Concise stability conditions for systems with static nonlinear feedback expressed by a quadratic program. *IET Control Theory Appl.*, 2(7):554–563, 2008.

[14] G. Li, D. P. Stoten, and J.-Y. Tu. Model predictive control of dynamically substructured systems with application to a servohydraulically actuated mechanical plant. *Control Theory Applications, IET*, 4(2):253 –264, 2010.

[15] T. Nakashima, H. Kato, and E. Takaoka. Development of real-time pseudo dynamic testing. *Earthquake Engineering and Structural Dynamics*, 21:79–92, 1992.

[16] A. R. Plummer. Model-in-the-loop testing. *Proc. IMechE Part I: Journal of Systems and Control Engineering*, 220:183–199, 2006.

[17] S. Skogestad and I. Postlethwaite. *Multivariable feedback control analysis and design*. John & Sons, Ltd, 2005.

[18] D. P. Stoten and R. A. Hyde. Adaptive control of dynamically substructured systems: the single-input single-output case. *Proc. IMechE Part I: Systems and Control Engineering*, 220:63–79, 2006.

[19] D. P. Stoten, J. Tu, and G. Li. Synthesis and control of generalised dynamically substructured systems. *Proc. IMechE Part I: Systems and Control Engineering*, 223:371–392, 2009.

[20] A. Syaichu-Rohman and R. Middleton. On the robustness of multivariable algebraic loops with sector nonlinearities. In *Decision and Control, 2002, Proceedings of the 41st IEEE Conference on*, volume 1, pages 1054 – 1059 vol.1, 10-13 2002.

[21] A. Syaichu-Rohman, R. H. Middleton, and M. M. Seron. A Multivariable Nonlinear Algebraic Loop as a QP with Application to MPC. In *European Control Conference*, Cambridge, 2003.

[22] A. R. Teel and N. Kapoor. The L_2 anti-windup problem: its definition and solution. In *Proc. 4th ECC*, Brussels, Belgium, 1997.

[23] M. C. Turner, G. Herrmann, and I. Postlethwaite. Incorporating robustness requirements into antiwindup design. *IEEE Transactions on Automatic Cotnrol*, 52, 2007.

[24] M. C. Turner and I. Postlethwaite. A new perspective on static and low order anti-windup synthesis. *International Journal of Control*, 77(1):27–44, 2004.

[25] M. J. Walsh, M. J. Hayes, and J. Nelson. Robust performance for an energy sensitive wireless body area network, an anti-windup approach. *International Journal of Control*, 86:59–73, 2009.

[26] P. F. Weston and I. Postlethwaite. Linear conditioning for systems containing saturating actuators. *Automatica*, 36:1347–1354, 2000.

[27] M. S. Williams and A. Blakeborough. Laboratory testing of substurctures under dynamic loads: an introductory review. *Phil. Trans. R. Soc. Lond. A*, 359:1651–1669, 2001.

[28] L. Zaccarian and A. R. Teel. A common framework for anti-windup, bumpless transfer and reliable designs. *Automatica*, 38(10):1735 – 1744, 2002.

[29] A. Zheng and M. Morari. Anti-windup using internal model control. *International Jounal of Control*, 60:1015–1024, 1994.